NUMERICAL SIMULATION OF SOLAR AND ASTROPHYSICAL MHD FLOWS

Jets, Loops, and Flares

KAZUNARI SHIBATA
National Astronomical Observatory
Mitaka, Tokyo 181, JAPAN
shibata@spot.mtk.nao.ac.jp

Abstract. The recent development of supercomputers enabled us to perform two or three dimensional MHD numerical simulations of dynamic phenomena in the solar atmosphere and in astrophysical gas layers. We are now able to compare simulation movies with real observational movies to clarify the origin of various dynamic phenomena such as jets, emerging magnetic loops, and flares. In this article, I will first summarize the difficulties and richness intrinsic to solar and similar astrophysical MHD simulations, and then show several examples of simulation results which answer various questions presented by old and new observations of solar and astrophysical MHD flows, in particular, in relation to jets, loops, and flares. The subjects treated in this article are solar jets (spicules and surges) accelerated by nonlinear MHD waves, astrophysical jets ejected from accretion disks via magnetic forces, the nonlinear evolution of the Parker instability in galactic and accretion disks, emerging magnetic loops in the solar atmosphere, magnetic reconnection driven by the Parker instability as a model of solar X-ray jets and compact flares, and finally magnetic reconnection in protostellar magnetospheres.

1. Introduction

In the latter half of this century, it has been revealed that our universe is full of active phenomena, such as jets ejected from active galactic nuclei (AGN), bipolar jets from young stellar objects (YSO) (e.g., Burgarella et al. 1993), various bursts in close binary systems, flares and coronal loops in the Sun and stars (e.g., Haisch et al. 1991), and so on. In the case of the solar phenomena, it has been established that magnetic fields play a dominant role in generating enormous activity in the solar atmosphere and

K. C. Tsinganos (ed.), Solar and Astrophysical Magnetohydrodynamic Flows, 217–247.

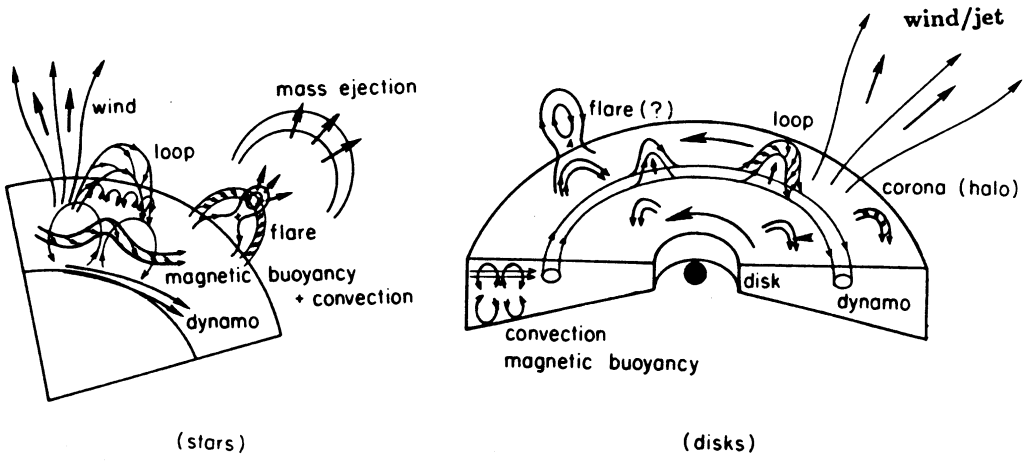

Figure 1. Schematic illustration of magnetic activity in stars and disks (accretion disks and galactic disks).

magnetohydrodynamics (MHD) is the basis for understanding macroscopic processes in these active phenomena (e.g., Parker 1979, Priest 1982). In the case of non-solar active phenomena, it has not yet been observationally established that magnetic fields are playing fundamental role, but recently many people began to recognize the importance of magnetic fields in astrophysical activity, such as in AGN and YSO's (e.g., Blandford 1993, Shu et al. 1987). In fact, recent developments in observations of radio and X-ray astronomy have revealed many active phenomena which are similar to solar magnetic phenomena as sketched in Fig. 1. Hence it is clear that MHD is the basis for understanding astrophysical magnetic activity, and for this reason, we have to solve the MHD equations.

As is well known, the MHD equations are a very complex set of nonlinear equations (e.g., Tsinganos et al. 1996). It is not easy to analytically solve them especially if we want to solve them in their full form (i.e., nonsteady, nonlinear, three dimensional, including non-ideal effects such as resistivity, viscosity, heat conduction, radiative cooling, and etc.). Even if spatial dimension is reduced to two or one, the equations are still complex enough to prevent analytical treatment, and only self-similar analytic solutions exist for axisymmetric systems (Blandford and Payne 1982, Tsinganos and Trussoni 1991, Tsinganos et al. 1993).

This is the reason why we have to perform numerical simulations using computers. Here, the word *numerical simulation* is defined as *to obtain numerical solutions of the time-dependent, nonlinear, MHD partial differential equations.*

It has been considered that theory and experiment are the two basic methods used in the physical sciences. The recent rapid development of

computers has changed this situation dramatically, and now we can say that *theory, experiment, and computer simulations* are the three basic methods used in the physical sciences.

This is also true in our field, *solar and astrophysical MHD.* Owing to recent development of supercomuters, it is now possible to perform two or three dimensional MHD numerical simulations of dynamic phenomena in the solar atmosphere and astrophysical gas layers, such as acceretion disks and galactic disks, in realistic situations. We are now able to compare simulation movies with real observational movies (in the case of the Sun) to explore the origin of various dynamic phenomena such as jets, emerging magnetic loops, and flares. If we succeed to reproduce the observed phenomena in computers, it would be possible to find some hints (and even physical conditions of enigmatic phenomena) which are not easy to be found by observations or experiments. When the observational data are so scarce, we can study basic physics by performing numerical experiment of basic physical processes by changing parameters extensively. It is easy to compare AGN jets with solar jets according to numerical experiment. Even an experiment (with unrealistic physical parameters) to understand basic physics is possible by using numerical experiment.

Consequently, the purposes of numerical simulations in solar and astrophysical MHD are two-fold :

(1) realistic modeling of observed phenomena,

(2) numerical experiment of basic physical processes.

In this article, starting from the discussion on the difficulties and richness intrinsic to solar and astrophysical MHD simulations, I will discuss many examples of simulation results which answer various questions presented by old and new observations of solar and astrophysical MHD flows, in particular, in relation to jets, loops, and flares, keeping above two purposes in mind.

2. Difficulties in Simulating MHD Phenomena in the Solar Atmosphere and Astrophysical Gas Layers

Since there are many excellent papers and books on the method of numerical simulations (e.g., Tajima 1989), I will not discuss details of numerical methods. Instead, I will discuss here some basic points in numerical solar and astrophysical MHD which have not been discussed in other papers and books.

The solar atmosphere and astrophysical gas layers (galactic and accretion disks) are *gravitationally stratified gas layers.* This is a very basic point of numerical solar and astrophysical MHD. Many difficulties (and richness)

in simulating solar and astrophysical MHD come from this point. There are essentially three basic properties of gravitationally stratified gas layer.

(1) *Large dynamic range in density (ρ), gas pressure (p_g), and $\beta(= p_g/p_{mag})$.* For example, the solar photosphere and chromosphere extends to more than $(10-15)H$, where

$$H = \frac{C_s^2}{\gamma g} = \frac{R_g T}{\mu g} \simeq 150\left(\frac{\mu}{1.2}\right)^{-1}\left(\frac{T}{6000\mathrm{K}}\right)\left(\frac{g}{g_\odot}\right)^{-1} \quad \mathrm{km}$$

is the pressure scale height in these (nearly isothermal) layers. Namely, the density decreases by more than $5-7$ orders of magnitude from the photosphere to the corona. Since the grid size in the vertical (z) direction should be less than $0.15-0.3H$, this means that we require many grid points ($> 50-100$) in the vertical direction. Large dynamic range in $\beta \sim {C_s}^2/{V_A}^2$ is a result of large dynamic range of sound speed C_s and/or Alfven speed V_A, which limits the time step Δt significantly through the CFL condition, $\Delta t < \Delta x/({C_s}^2 + {V_A}^2 + V^2)^{1/2}$, when we use explicit scheme.

(2) *Wave amplification through vertical propagation.* Since the density decreases rapidly with height, the amplitude of an MHD wave increases with height when the wave propagates from the bottom of the atmosphere to the top. For example, the energy flux carried by an acoustic wave (or a slow mode MHD wave) propagating along the vertical magnetic flux tube with cross section A becomes $\rho {V_\parallel}^2 C_s A =$ constant, if the WKB approximation holds. From this, we find

$$V_\parallel \propto \rho^{-1/2} A^{-1/2}$$

since the temperature is nearly constant in the photosphere and chromosphere within a factor of 2. Hence if $A_{cor}/A_{ph} \sim 100$ (typical value for the ratio of the cross-section of a flux tube in the photosphere, A_{ph}, to that in the corona, A_{cor}, in the quiet region of the Sun) and $\rho_{tr}/\rho_{ph} = 10^{-6}$, the amplitude of the acoustic wave (or slow mode) is enormously amplified by 2 orders of magnitude, say from 1 km/s in the photosphere to 100 km/s in the transition region if the wave remains a linear wave, where ρ_{tr} and ρ_{ph} are the densities of the transition region and photosphere, respectively. (Actually, nonlinear effects and the associated dissipation become important in the upper layer. See next section.) Note that in the case of MHD waves, approximate one dimensional propagation along the flux tube is realized (for slow mode and Alfven mode), so that the wave amplification is stronger than in the case of non-magnetic acoustic waves (e.g., Shibata 1983).

(3) *Various instabilities driven by gravitational energy.* In a gravitationally stratified gas layer, various instabilities occur owing to gravitational

free energy, such as convective instability, Rayleigh-Taylor instability, magnetic buoyancy instability, Parker instability, etc. These instabilities and resulting mass motion generate various MHD waves and electric currents, which could be the source of energy to heat the chromosphere and corona. Even a more vigorous activity such as flares could be a result of release of magnetic free energy which is stored by dynamo action and/or interaction of a flux tube with turbulent motion in the convection zone. Note that the magnetic field significantly enhances the activity of gravitationally stratified gas layers through *coupling with convection and rotation* and *magnetic buoyancy* (Parker 1979).

All these three factors introduce various difficulties in actual numerical simulations. For example, even a small numerical error at the bottom of the atmosphere can be amplified enormously in the upper atmosphere, and can affect the dynamics seriously. Hence the treatment of the lower boundary is the most important in this kind of numerical simulations. Various physical instabilities should be discriminated from numerical instabilities, and thus we must be well aware of the physics of these instabilities.

On the other hand, these factors introduce richness (and interesting physics) to the problem. Enormously amplified waves can accelerate a jet along the tube and can heat the atmosphere. Magnetic flux loops rapidly emerge from below the photosphere to the corona, and interact with ambient fields, leading to violent reconnection and jets.

These vigorous activity intrinsic in a gravitationally stratified magnetized gas layers, in turn, introduce another kind of numerical difficulties; i.e., strong MHD waves are generated by these active phenomena. These waves are reflected at the numerical boundary, which often produces physical/numerical resonances near the upper boundary, leading to numerical instability. Hence, the treatment of the upper boundary is also one of the most important (and difficult) problems in numerical solar and astrophysical MHD. There are a number of methods to overcome this difficulty, though there is no almighty one. The simplest and the safest "method" is to move the upper boundary as far as possible using non-uniform grids, which physically eliminates the chance of wave reflection.

3. Jets – Plasma Acceleration due to Nonlinear MHD Waves and Centrifugal Force

3.1. SOLAR JETS: SPICULES AND SURGES

3.1.1. *Slow Shock Acceleration*

As we discussed in the previous section, a small amplitude slow mode MHD wave (acoustic wave along a flux tube) grows enormously during the prop-

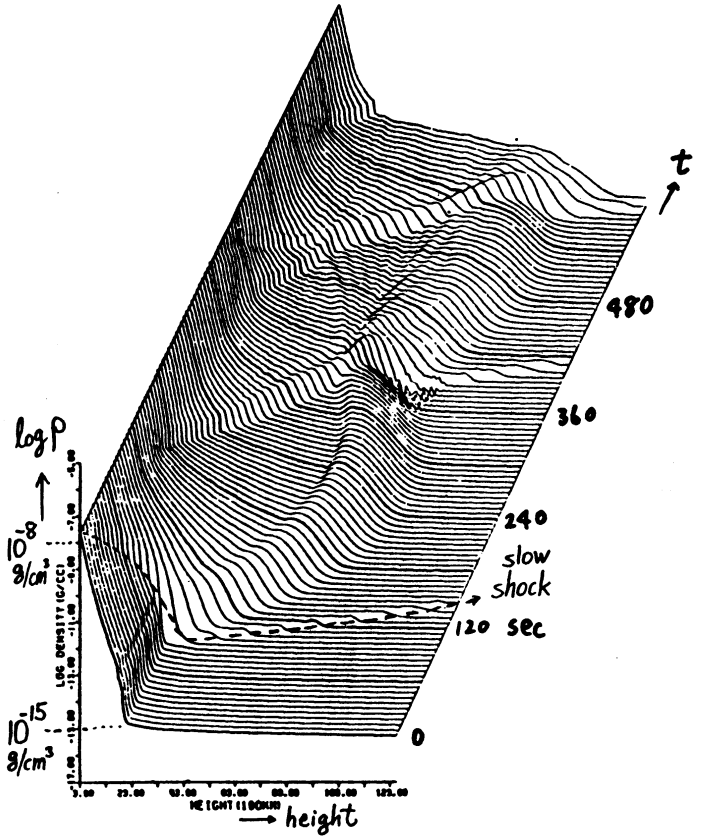

Figure 2. Spicule model by Suematsu et al. (1982). The density distribution is shown as a function of height and time. Note that the slow mode wave (acoustic wave in a flux tube) grows as it propagates upward and finally collides with the transition region, creating a spicule-like ejection.

agation along a vertical flux tube because of steep density gradients in these atmospheres. Even if the original velocity amplitude is well below the sound speed at the photospheric level, the velocity amplitude can easily exceed the sound speed in the chromosphere, and the wave can evolve into a shock. Once the shock is created, it can decay and heat the chromosphere. This is essentially the same as the scenario of classical acoustic shock coronal/chromospheric heating theory (e.g., Ulmschneider et al. 1991 for a review). The slow shock finally collides with the transition region (a kind of contact discontinuity) to accelerate the transition region as well as chromospheric plasmas in the upward direction. Such a chromospheric ejection might correspond to a spicule.

This scenario was first proposed by Osterbrock (1961), and was confirmed later by Suematsu et al. (1982) by performing full nonlinear 1D simulations (Fig. 2). In the simulation model of Suematsu et al. (1982), it was assumed that a sudden pressure enhancement due to a small flare-like bright point at the footpoint of spicules generates slow mode waves which eventually become shocks and accelerate spicules.

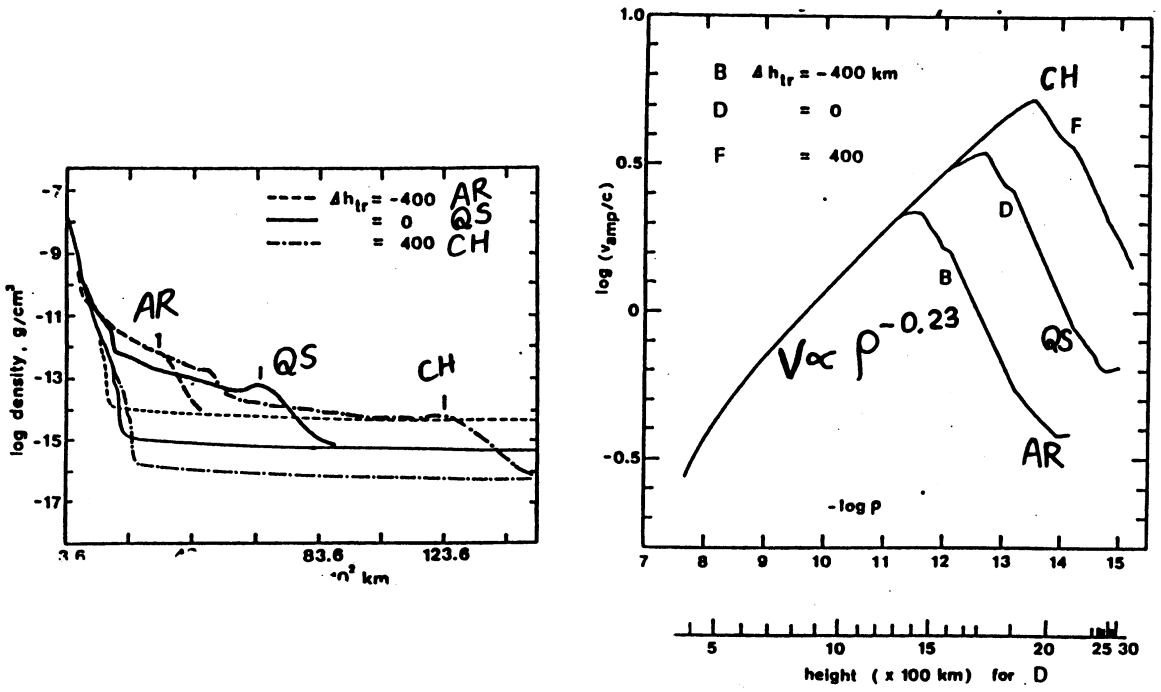

Figure 3. Right: Growth of a slow shock for various atmospheres with different transition region heights (Shibata and Suematsu 1982). Left: Density distribution in height for three "spicule" models with different initial transition region heights.

Shibata et al. (1982) showed that if the sudden pressure enhancement occurs above the middle chromosphere, the jets are directly accelerated by the *pressure gradient force* in the pressure enhancement region, not by the shock (see also Sterling et al. 1993 for the effect of radiation and conduction). In other words, if the sudden pressure increase (or energy release) occurs *below the middle chromosphere*, the jets are accelerated by the *slow shock*, not by the pressure gradient force in the energy release region. This can be also applied to other acceleration mechanisms, such as magnetic acceleration, if it occurs in the photosphere. That is, if the sudden plasma acceleration occurs *along the global flux tube* in the photosphere, the final jets ejected into the corona are not the jets accelerated in the photosphere, but those accelerated in the upper chromosphere by the *slow shock* which is generated by the plasma flow in the photosphere and has propagated to the upper chromosphere.

Shibata and Suematsu (1982) extended this model (*bright point - slow shock* model) to the cases of different initial transition region heights, and showed that spicules are taller in coronal holes and shorter in active regions; in the latter case, the height is so small that the ejection cannot be regarded as spicules. These theoretical predictions nicely fit with the observations that spicules are tall in polar coronal holes and absent in active region plages (Shibata and Suematsu 1982). The physical reason of this is as follows; (1) the rate of increase in velocity amplitude of strong shocks is $V_{||} \propto$

$\rho^{-0.23}$ (Shibata and Suematsu 1982), and (2) the density ratio between the photosphere and the corona (ρ_{ph}/ρ_{co}) is larger in coronal holes and smaller in active regions than in quiet region (Fig. 3).

Hollweg (1982) proposed a similar but slightly different idea, i.e., the *rebound slow shock model* in which spicules are repeatedly accelerated by multiple shocks originating from the wake oscillating at the acoustic cut off frequency (see also Sterling and Hollweg 1988).

It is interesting to note that the physics of slow shock propagation discussed above is basically the same as that of shock propagation in type II supernova explosion (e.g., Ohno et al. 1961, Colgate and White 1967). The only difference is that the former is confined in a magnetic flux tube, but the latter is a spherical shock propagation.

3.1.2. *Nonlinear Alfven Wave (or Magnetic Twist) Acceleration*

Similarly to the slow mode, the amplitude of the Alfven mode also grows during the propagation along the vertical flux tube. In this case, from the conservation of energy flux $\rho V_\perp{}^2 V_A A$ = constant (WKB approximation) and $A \propto 1/B$, the amplitude $V_\perp$ becomes

$$V_\perp \propto \rho^{-1/4}.$$

Nonlinearity $V_\perp/V_A$ is then

$$V_\perp/V_A \sim B_\perp/B \propto \rho^{1/4} B^{-1}.$$

For the quiet solar atmosphere ($\rho_{tr}/\rho_{ph} \sim 10^{-5}, B_{tr}/B_{ph} \sim 10^{-2}$), we find that $V_{\perp,tr}/V_{\perp,ph} \sim 20$, $(V_\perp/V_A)_{tr}/(V_\perp/V_A)_{ph} \sim 5$. Thus a linear Alfven wave can evolve into a nonlinear wave if the flux tube expands significantly like a solar flux tube in a quiet region.

If the nonlinearity becomes important, the magnetic pressure force $\nabla(B_\perp{}^2/8\pi)$ can push the plasma parallel to the unperturbed flux tube, so that the plasma can be accelerated along the global flux tube. In other words, the nonlinear magnetic pressure force generates longitudinal plasma motion or a slow mode MHD wave. In the case of the nonlinear torsional Alfven wave (Hollweg et al. 1982, Shibata and Uchida 1985), not only the magnetic pressure force but also the centrifugal force $\rho V_\perp{}^2/r$ can accelerate the plasma along the global flux tube, where r is the radius of the flux tube.

Hollweg et al. (1982) studied the nonlinear propagation of torsional Alfven waves along the vertical (expanding) magnetic flux tube from the photosphere to the corona, by performing 1.5D MHD nonlinear simulations. They found that a spicule-like chromospheric ejection is generated when a large amplitude nonlinear torsional Alfven wave (equivalent to switch-on fast shock in this geometry) collides with the transition region. This

process is similar to that in the case of the collision of a slow shock with the transition region (Fig. 2 and Shibata et al. 1982). (See also later related works by Mariska and Hollweg 1985, Hollweg 1992).

Shibata and Uchida (1985) studied the plasma acceleration associated with the sudden relaxation and propagation of the nonlinear magnetic twist, and applied the results to solar surges. They proposed that such sudden relaxation of nonlinear magnetic twist would be possible if the reconnection occurs between an untwisted flux tube and a twisted flux tube (Shibata and Uchida 1986b). On the other hand, if the magnetic twist is generated continuously by the interaction of the accretion disk with global poloidal magnetic fields, a similar magnetic twist jet would be produced and might explain astrophysical jets ejected from accretion disks. This *sweeping-magnetic-twist* jet model for astrophysical jets has been developed by Shibata and Uchida (1986a, 1987, 1990) incorporating the effects of accretion disk, and is applied to bipolar molecular flows in star forming regions by Uchida and Shibata (1985), which will be discussed in detail in the next subsection.

3.2. ASTROPHYSICAL JETS EJECTED FROM ACCRETION DISKS

3.2.1. *Nonsteady MHD Jets from Thin Disks - The Sweeping Magnetic Twist Mechanism*

If a strong poloidal magnetic field penetrates an accretion disks, what would occur ? Shibata and Uchida (1986a, 1987, 1990) studied this problem in detail as an initial value problem (see Figs. 4 and 5), and the results have been applied to bipolar molecular flows in star forming regions (Uchida and Shibata 1985). The initial condition of their model is as follows. A geometrically thin disk (with $(C_s/V_k)^2 \sim 10^{-2} - 10^{-3}$) is rotating around a point mass at the center. A uniform magnetic field (with $(V_A/V_k)^2 \sim 10^{-2} - 10^{-3}$) penetrates the disk vertically, and there is a non-rotating hot corona outside the disk. In the disk, the ratio of rotational velocity to the Keplerian velocity is taken to be a free parameter including both Keplerian and sub-Keplerian cases ($V_\varphi/V_k = 0.6 - 1.0$). In the Keplerian case, the rotating disk pulls the poloidal field lines toward the azimuthal direction, generating toroidal fields which propagate along the poloidal field lines as torsional Alfven waves. This process extracts angular momentum from the disk (i.e., *magnetic braking*), and hence the disk begins to contract, eventually producing bipolar jets when the toroidal fields get strong enough. In the sub-Keplerian case, these processes become more vigorous because the generation of toroidal fields is stronger and faster. Figures 4 and 5 show one typical example of such sub-Keplerian case. Note that the essential point of this process is independent of whether the rotaional velocity of the disk is Keplerian or not.

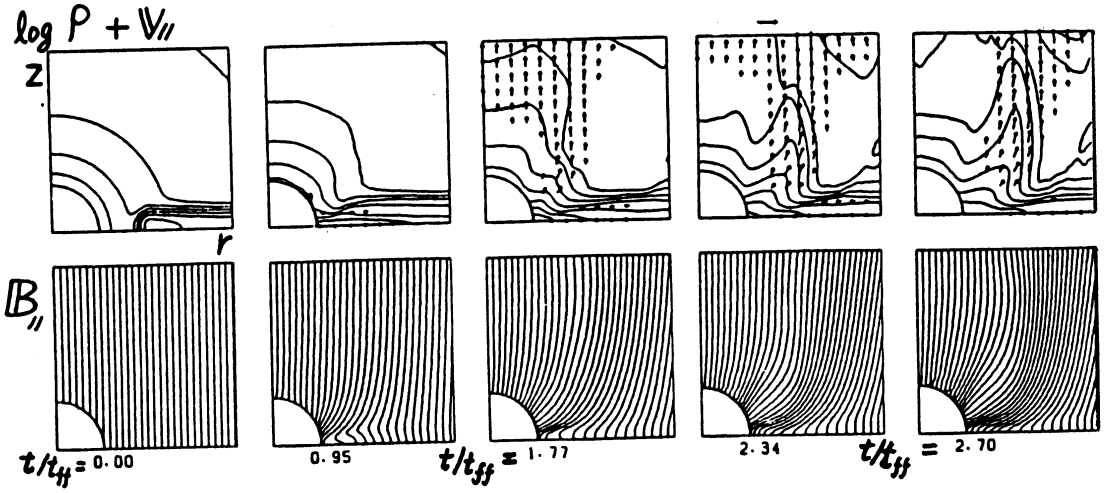

Figure 4. *Sweeping magnetic twist* jet model for astrophysical jets ejected from an accretion disk (Shibata and Uchida 1986a). (a) Density and velocity, (b) poloidal magnetic field lines. The times are in units of the free fall time at the inner edge of the initial disk.

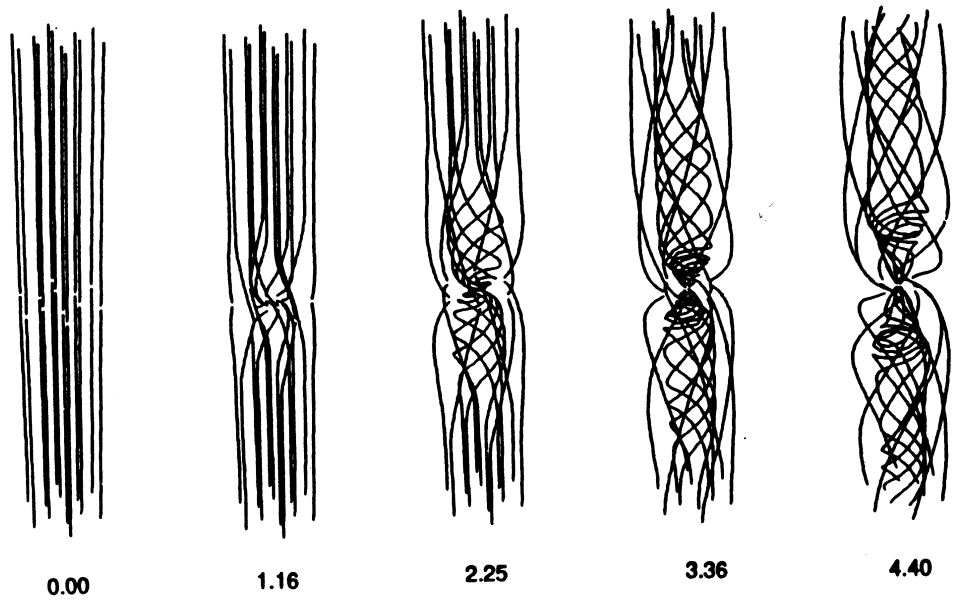

Figure 5. 3D representaion of magnetic field lines in the *sweeping-magnetic-twist* jet model (Shibata and Uchida 1990). The times are in units of the free fall time at the inner edge of the initial disk.

The acceleration of the jet is due to the $\mathbf{J} \times \mathbf{B}$ force (magnetic pressure gradient force $\nabla B_\varphi{}^2/8\pi$) and centrifugal force. This jet is a nonsteady version of a magneto-centrifugally driven wind/jet (e.g., Blandford and Payne 1982, Pudritz and Norman 1986). The jet has a hollow cylindrical shell structure with a helical motion in it, and these characteristics were actually found in the L1551 bipolar molecular flows (Uchida et al. 1987; though see Moriaty-Schieven and Wannier 1991 for a different interpretation) and

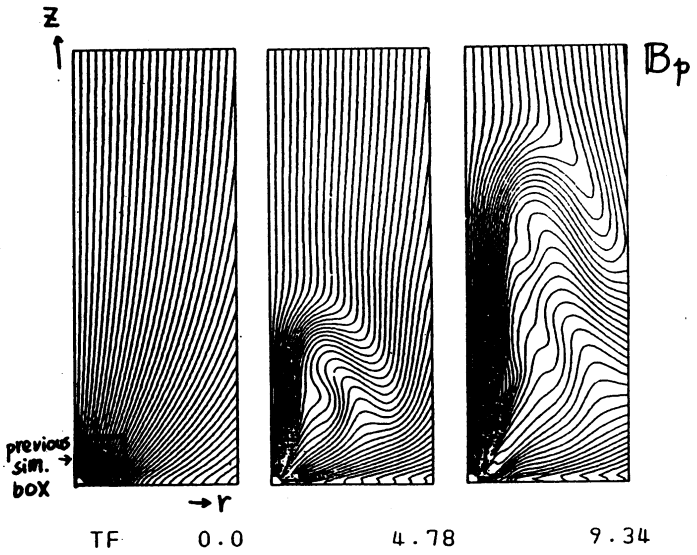

Figure 6. Large scale behavior of a *sweeping-magnetic-twist* jet when a jet propagates into diverging magnetic fields. Note the vigorous collimation by the toroidal fields. The times are in unit of the free fall time at the inner edge of the initial disk. A small square box in the left bottom corner of the $t = 0$ figure is the simulation box adopted by Shibata and Uchida (1986a).

in the Galactic center radio lobes (Sofue and Handa 1984, Uchida, Shibata, Sofue 1985, Shibata and Uchida 1987). The velocity of the jets produced by this mechanism is comparable to the Keplerian velocity at the footpoints of the jet, $V_{jet} \sim (1-2)V_k$, and is in proportion to $B^{0.5-0.7}$. [1] The latter is similar to Michel's minimum energy solution (Michel 1969)

$$V_\infty \sim (\Omega^2 B^2 R^2/\dot{M})^{1/3} \propto B^{2/3},$$

where R is the radius of the disk at the footpoints of the jet.

Near the disk, the collimation of the jet is due to the poloidal field. If the initial poloidal field diverges at a larger distance, however, the effect of the toroidal field increases as the jet propagates farther, and eventually collimates the jet (Fig. 6). This is the same as in the collimation of a centrifugally driven jet/wind (Sakurai 1987, Heyvaerts and Norman 1989, Sauty and Tsinganos 1994).

3.2.2. *Relation to the Magneto-Rotational (Balbus-Hawley) Instability*

Stone and Norman (1994) studied the same problem as that of Shibata and Uchida (1986a), and confirmed the basic points on the production of jets.

[1] Sauty and Tsinganos (1994) also found $V_{jet} \sim (1-2)V_k$ in somewhat different situations.

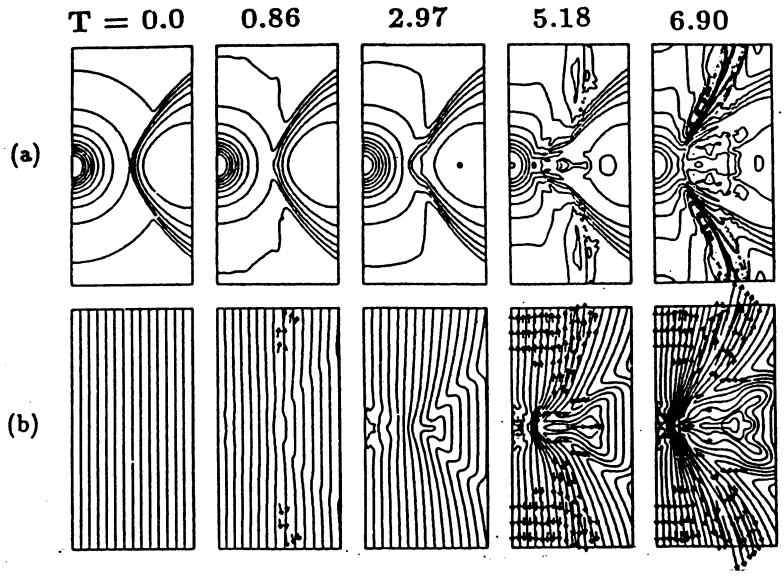

Figure 7. *Sweeping magnetic twist jet* ejected from a thick disk (Matsumoto et al. 1996a). The times are in units of the free fall time at the inner edge of the initial disk.

The new feature they found is the magneto-rotational instability (Balbus and Hawley 1991) when the initial magnetic field is weak. [2]

It is interesting to note that some of the key features of this magneto-rotational instability, such as the avalanche (accretion) flow at the surface of the disk, have already been seen in some results of Shibata and Uchida's simulations (1986, 1987, 1990) as well as in the early results of Matsumoto et al.'s simulations of magnetized thick disks before 1990 (see below). Although this feature was physically understood at that time, it has unfortunately never been explicitly emphasized nor been studied in detail. This is because the spatial resolution of these simulations was not good enough. ¿From this history, we can learn that we have to consider numerical results more seriously even if the spatial resolution is not so good. There are a lot of hints in numerical simulation results from which we can develop important theories.

3.2.3. *Nonsteady MHD Jets from Thick Disks*

In order to develop an AGN jet model, Matsumoto et al. (1996a) studied the case of thick disks penetrated by the poloidal field, by performing nonsteady 2.5D MHD simulations similar to Shibata and Uchida (1986a). Their results (see Fig. 7) show; (1) Avalanche (accretion) flow occurs along the surface of thick disks. (2) Magneto-rotational instability (Balbus and Hawley 1991)

[2]It may be said that even the basic physics of nonsteady MHD jet-accretion (Shibata and Uchida 1986a, Stone and Norman 1994) is the same as that of the Balbus-Hawley (1991) instability.

occurs inside thick disks. (3) The velocity of jets is again comparable to the Keplerian velocity, $V_{jet} \sim 0.6 - 2.3V_k \propto B^{0.15-0.25}$ if initially $(V_A/V_\varphi)^2 < 10^{-3}$. (4) The mass loss rate by the jet $\dot{M}$ is in proportion to the magnetic field strength; $\dot{M} \propto B$.

3.2.4. *Relation between Nonsteady and Steady Jets*

What is the relation between these nonsteady MHD jets and steady magnetically driven jets (such as in Blandford and Payne 1982) ? In order to answer this question, Kudoh and Shibata (1995) studied one dimensional (1.5D) steady magnetically driven jets along a fixed poloidal field line for a wide range of parameters, assuming the shape of the poloidal magnetic field line. There are two free parameters in their problem;

$$E_{mg} = \left(\frac{V_A}{V_k}\right)^2 \simeq 3.8 \times 10^{-4} \left(\frac{B}{1\mathrm{G}}\right)^2 \left(\frac{M}{M_\odot}\right)^{-1} \left(\frac{n}{10^{12}\mathrm{cm}^{-3}}\right)^{-1} \left(\frac{R}{15R_\odot}\right),$$

$$E_{th} = \frac{1}{\gamma}\left(\frac{C_s}{V_k}\right)^2 \simeq 6.5 \times 10^{-3} \left(\frac{T_d}{10^4\mathrm{K}}\right) \left(\frac{M}{M_\odot}\right)^{-1} \left(\frac{R}{15R_\odot}\right),$$

where V_A is the Alfven speed based on the poloidal field, and the physical values in these equations are suitable for protostellar jets. They found that the inclination angle of poloidal magnetic field lines at the surface of accretion disks is very important to determine the properties of the jet as first noted by Blandford and Payne (1982) and later stressed by Cao and Spruit (1994). As the angle between the poloidal field and the disk surface decreases, the mass flux of the jets increases. If the angle becomes less than 60 degrees, a high mass flux jet with strong toroidal fields can arise, depending on the poloidal field strength. Namely, in such low angle case, the solution can be generally classified into two branches,

(1) *centrifugally driven jet,*

(2) *magnetic pressure driven jet.*

The former arises when the poloidal field is strong, i.e., the poloidal field is dominant near the surface of the disk, whereas the latter arises when the poloidal field is weak, i.e., the toroidal field is dominant near the disk (Fig. 8). In the former case, the main acceleration occurs below the Alfven point by the centrifugal force, whereas in the latter the acceleration occurs above the Alfven point by the magnetic pressure force of the toroidal field. The latter branch corresponds to the steady MHD jet model developed by Lovelace et al. (1991; see also related 2.5D work by Ustyugova et al. 1995). In the case of a *magnetic pressure driven jet*, (i.e., $E_{mg} < 0.01$), Kudoh and Shibata (1995) found;

(1) the mass loss rate is in proportion to the magnetic field strength, i.e.,

$$\dot{M} \propto {E_{mg}}^{0.5} \propto B,$$

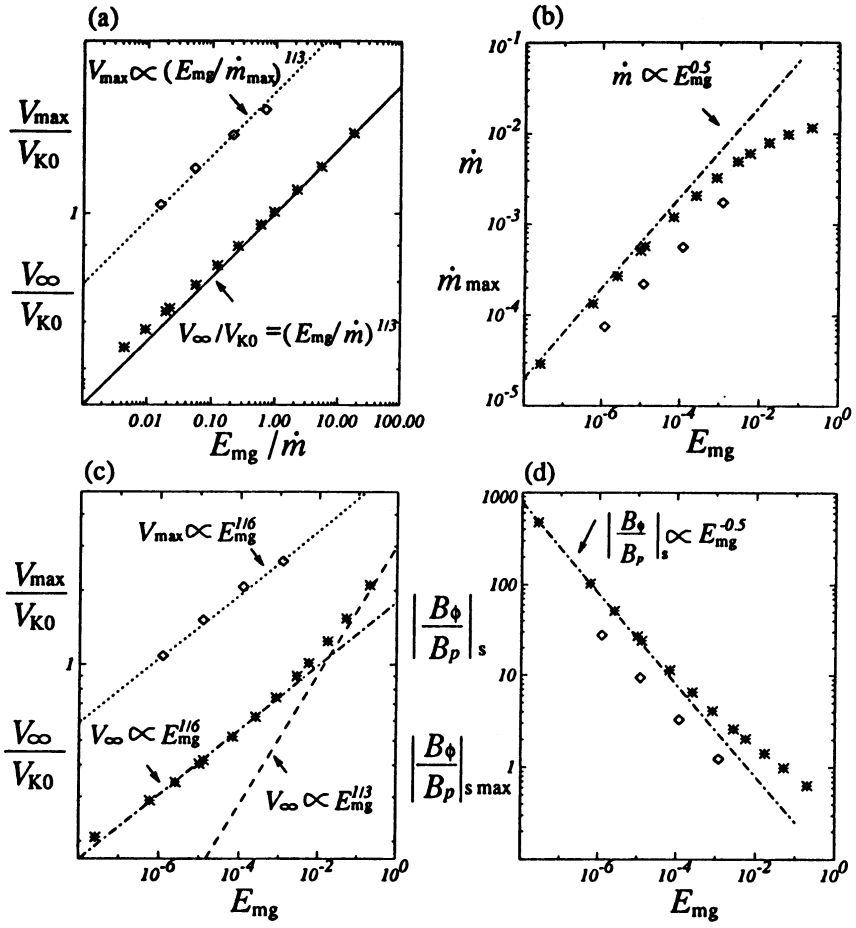

Figure 8. 1.5D steady and nonsteady magnetically driven jet models developed by Kudoh and Shibata (1995, 1996a,b). (a) Terminal velocity for steady case (asterisk) and maximum velocity for nonsteady case (diamond) as a function of $E_{mg}/\dot{m}$, where $\dot{m}$ is normalized by $\rho_d V_k R^2$. The solid line shows Michel's minimum energy solution. (b) The normalized mass flux versus E_{mg}. (c) Terminal (or maximum) velocity as a function of E_{mg}. (d) The ratio of the toroidal field to the poloidal field at the slow point, B_φ/B_p, versus E_{mg}. In these figures, the steady solution is denoted by asterisks, and the nonsteady solution is shown by diamonds.

(2) the terminal velocity V_∞ of the jet becomes Michel's minimum energy solution, but the dependence of V_∞ on B is weaker than had been thought for a centrifugally driven jet because of $\dot{M} \propto B$;

$$V_\infty \propto (E_{mg}/\dot{M})^{1/3} \propto B^{1/3},$$

(3) the terminal velocity is of the order of Keplerian velocity at the footpoint of the jet for a wide range of parameters; $V_\infty \propto 0.5 - 4.0 V_k$ for $10^{-5} < E_{mg} < 0.1$.

These results explain the simulation results of Matsumoto et al. (1996a) very well, and explain also previous 2.5D nonsteady MHD simulations (Shibata and Uchida 1986a, 1987, 1990, Stone and Norman 1994) which showed

that the velocity of the nonsteady jet is of the order of the Keplerian velocity and the toroidal magnetic field is dominant near the disk. [3]

On the basis of these results, Kudoh and Shibata (1995) predicted the physical condition of the disk from which YSO optical jets and/or high velocity neutral winds are ejected. Namely, the jet production radius must be less than 20 $R_\odot$ (for one solar mass protostar) to explain the velocity of optical jets and/or high velocity neutral wind, and magnetic field strength > 3 G, and the temperature must be larger than 3000 K at $r \simeq 20R_\odot$.

Using the same poloidal field line configuration, Kudoh and Shibata (1996a,b) further studied nonsteady 1.5D MHD simulations assuming the initial and boundary conditions similar to those of Shibata and Uchida (1986a) to see the relation between nonsteady jets and steady jets. Note that the boundary condition of this problem is not suitable to get steady solutions. Nevertheless, such boundary conditions are adopted to see the long term behavior of the Shibata-Uchida simulation model. Note also that still at present it is not easy to perform long term 2.5D MHD simulations of this model. Although the boundary conditions are not suitable to get steady solution, Kudoh and Shibata found that the solution show some characteristics of the steady solution in the early stages of evolution, around 10 orbital periods. When the magnetic field is weak, the positions of Alfven and slow points agree well with those of the steady solution. Even in the cases where these positions do not agree with those of the steady solution, the dependences of maximum velocity and mass loss rate of jets upon E_{mg} agree with those found in the steady solution. Since the dynamics of 1.5D MHD model are common with that of 2.5D MHD model except for the accretion, we can say that characteristics of nonsteady jets found in 2.5D MHD models are essentially similar to those of the steady models. For example, the maximum velocity of jets found in 2.5D MHD model ($V_{jet} \sim 1 - 2V_k$) is explained by the steady models very well.

3.2.5. *Three Dimensional Propagation of MHD Jets*

Todo et al. (1993) have studied the stability of MHD jets by performing three dimensional MHD simulations. In their model, a jet was assumed initially to be propagating along helically twisted flux tube. The initial helical field is force free and stable to the kink instability. A dense region is located somewhere ahead of the jet, and the subsequent interaction of the helical jet with the dense region was studied in detail. (See Todo et al. 1992 for the 2.5D version, and Uchida et al. 1992 for the 1.5D version.) It was found that

[3]Exactly speaking, the results of Shibata and Uchida (1986a) are an intermediate case between *centrifugally driven jets* and *magnetic pressure driven jets*, and hence V_{jet} showed stronger dependence on B than in a pure magnetic pressure driven jet.

the collision of the *magnetic-twist-jet* with the dense region produce strong magnetic twists ($B_\varphi \gg B_z$) (see also Shibata and Uchida 1990) which eventually become unstable to the kink instability in three dimensional space. The resulting magnetic field and velocity field configurations are similar to those observed around the filamentary sructures seen in some HH objects in star forming regions (Todo et al. 1993).

4. Loops – Nonlinear Evolution of the Parker Instability

4.1. MAGNETIC LOOPS IN GALACTIC AND ACCRETION DISKS

4.1.1. *Typical Nonlinear Evolution of the Parker Instability: The Most Unstable Mode*

The *Parker instability* is the undular mode of *magnetic buoyancy instability* (Hughes and Proctor 1988). It occurs when the gas layer, which is supported by horizontal magnetic field against gravity, is perturbed to undulate (Parker 1966, 1979; see Mouschovias 1996 for an elementary explanation). It occurs also for the horizontal isolated flux tube embedded in the non-magnetized plasmas (e.g., Moreno-Insertis 1986, Schüssler 1995).

Matsumoto et al. (1988) have first peformed full nonlinear 2D simulations of the Parker instability. They considered a local part of the gas disk rotating around a point mass M. Taking a local cartesian coordinate (x, z), with x in the azimuthal direction and z in the vertical direction, they assumed that the magnetic field is initially parallel to the equatorial plane (in the x direction). It is further assumed that the magnetized gas layer is isothermal and is in magneto-hydrostatic equilibrium with uniform Alfven and sound speeds. The pure 2D perturbations ($k_y = 0$, where k_y is the wavenumber perpendicular to the magentic field lines) are considered and the effects of rotation, Coriolis force, and cosmic rays are all neglected. Ideal MHD with an isothermal equation of state is assumed.

Figure 9 shows a typical example of the simulation results in the case of the most unstable mode with parameters $\epsilon = (GM/R)/\ [(1+1/\beta){C_s}^2] = 6$, $\beta = 8\pi p/B^2 = 1$. In this case, the periodic boundaries are assumed at $x = 0$ and $x = X_{max}$ and the small periodic undular perturbation was given. As the instability develops, the gas slides down the rising magnetic loop, forming a dense structure in the valley. Note that the perturbed magnetic field lines cross the equatorial plane of the disk as predicted by the linear stability theory (Horiuchi et al. 1988, Giz and Shu 1993). The growth of the perturbation is saturated when the maximum velocity of downflow becomes comparable to the initial Alfven speed V_A. The maximum velocity of the rising motion of the magnetic loop is $0.3 - 0.5 V_A$. In this case, since the Alfven speed is larger than the sound speed (because initial $\beta = 2(C_s/V_A)^2 = 1$),

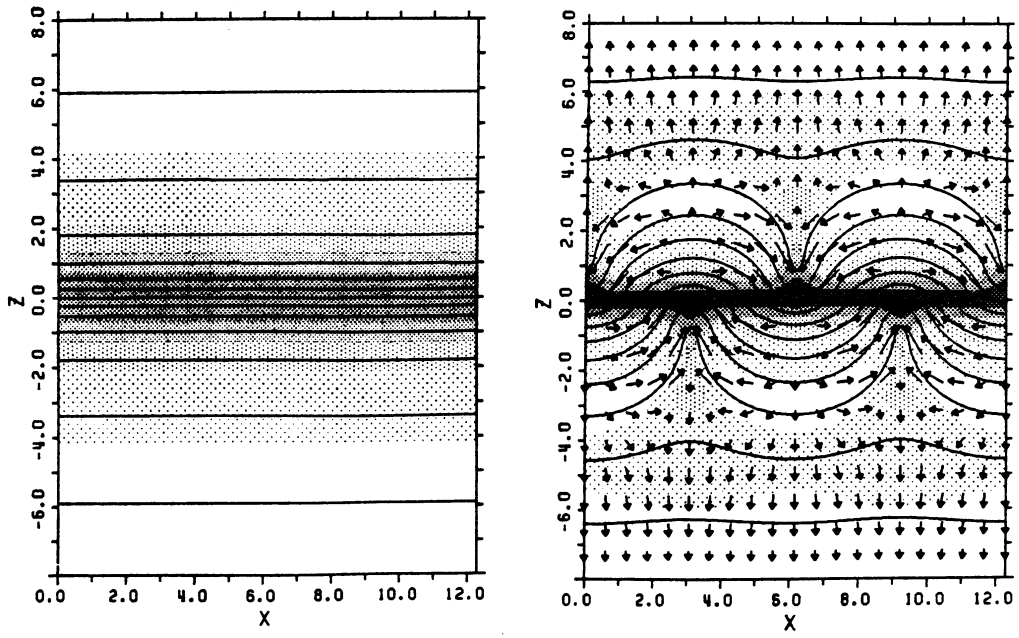

Figure 9. Left: Initial condition. Right: The nonlinear evolution of the Parker instability at $t/\tau = 5.99$, where τ is the linear growth time (Matsumoto et al. 1988). Distribution of density (grey scale), mangnetic field lines (solid curves) and velocity fields (arrows).

the downflow becomes supersonic (i.e., $V_{downflow} \sim V_A > C_s$), forming shock waves in the valley of the undulating field lines. This shock wave gradually propagates upward along the magnetic field line. After passing the shock, the downflow gas settles into a quasi-magneto-hydrostatic equilibrium state (Mouschovias 1974), forming a giant moledular cloud. (Similar results are obtained by Basu, Mouschovias, and Paleologou 1996.) On the other hand, if initial Alfven speed is less than the sound speed (e.g., $\beta = 10$), the downflow does not become supersonic so that the system does not reach the quasi static equilbrium state but undergoes nonlinear oscillation.

Whether shock waves occur or not is determined by whether the initial Alfven speed is larger than the sound speed or not, since the maximum speed of the downflow is comparable to the initial Alfven speed. Why is the downflow speed comparable to the initial Alfven speed ? The reason is as follows. The energy of the downflow comes from the gravitational potential energy stored initially in the magnetically supported gas layer, i.e., $gH \sim {C_s}^2 + {V_A}^2/2$. Since the plasmas settle into quasi-hydrostatic equilibrium along the curved magnetic loop, the final gravitational energy is written as $gH' \sim {C_s}^2$. Hence

$$ {V_{downflow}}^2/2 \sim g(H - H') \sim {V_A}^2/2, $$

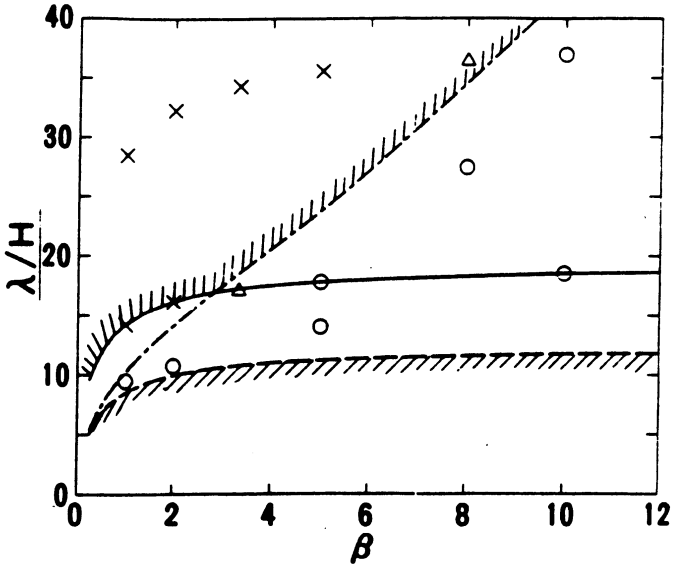

Figure 10. The parameter space for the *shock wave formation* (crosses) and the *nonlinear oscillation* (circles) (Matsumoto et al. 1990). This figure shows the wavelength λ vs. $\beta = p_g/p_{mag}$. The solid curve shows the most unstable wavelength, and the dash-dotted curve denotes λ_s (see the text). The dashed curve shows the critical wavelength of the linear Parker instability.

which leads to $V_{downflow} \sim V_A$. Note that this result is applicable only to the most unstable modes. If the instability occurs for longer wavelength modes, the downflow speed becomes larger (see Matsumoto et al. 1990 and next subsection).

4.1.2. *Condition of Shock Wave Formation and Nonlinear Oscillation*

In order to clarify the condition of shock wave formation and nonlinear oscillation in general situations, Matsumoto et al. (1990) have studied the effect of initial horizontal wavelength, λ. They adopted $\epsilon = 6$ model which corresponds to $p(z = \infty)/p_{disk} \simeq 2 \times 10^{-3}$, and studied various cases with $\lambda \neq \lambda_{max}$, where λ is the most unstable wavelength. They found (see Fig. 10) that

(1) If $\lambda > \lambda_s = (3.5\beta + 6)\Lambda$, shock waves are formed, and the system evolves into the quasi-static state, whereas if $\lambda < \lambda_s$, the nonlinear oscillation occurs. [4] Here $\Lambda = C_s{}^2(1 + 1/\beta)/g_{max}$.

(2) Once the nonlinear oscillation occurs, the nonlinear mode coupling occurs between different wavelength modes, increasing the wavelength of the perturbation with time up to λ_s. Hence eventually shock waves are formed, and the system evolves into the quasi-static equilibrium state. Note

[4]Note that this critical wavelength λ_s is different from the crtical wavelength λ_c for the linear Parker instability. This wavelength, λ_s, is determined by the nonlinear effect.

that this wavelength is longer than the linearly determined most unstable wavelength.

Summarizing these results, the length of magnetic loops in final equilibrium state is rougly given by $\max(\lambda_s, \lambda_{max})$, i.e.,

$$\lambda_{loop} \simeq \begin{cases} 6\pi[\beta/(\beta+2)]^{1/2}\Lambda = 6\pi(\beta+1)\beta^{-1/2}(\beta+2)^{-1/2}H, & (\text{ for } \beta < 3) \\ (3.5\beta+6)\Lambda = (3.5\beta+6)(1+1/\beta)H, & (\text{ for } \beta > 3) \end{cases}$$

where $H = {C_s}^2/g_{max}$ and $g_{max} = 0.385GM/R^2$. When applying this result to the actual accretion disk and galaxies, we can assume that H approximately corresponds to the thickness of the disk when $\beta > 1$. This result would be important to estimate the actual length of magnetic loops produced by the Parker instability in accretion disks and galactic disks.

4.1.3. *Effect of Corona (Halo)*

There is now increasing observational evidence that there is a hot corona around various astrophysical objects, such as stars, accretion disks, galactic disks, and so on. What is the effect of the corona upon the linear and nonlinear evolution of the Parker instability ? In the corona, the temperature is high so that the pressure scale height, H, is larger than that in the lower layer (disk or photosphere/chromosphere). Since the critical wavelength and the most unstable wavelength of the Parker instability are in proportion to H (Parker 1966, 1979), this means that the most unstable wavelength in the low temperature layer becomes *stable* in the corona. Consider the disk (either accretion disk or galactic disk) with a hot corona above and below it, and assume that the base height of the corona is $|z_{corona}|(> H)$ above/below the equatorial plane $z = 0$. Since the corona is stable for the most unstable wavelength in the disk, the instability is confined inside the disk, i.e., the effective wavelength in the vertical direction λ_z becomes comparable to z_{corona}. When λ_z decreases, the growth rate of the instability decreases and also the critical and most unstable wavelengths increase. Kamaya et al. (1996b) studied these points in detail.

It should be emphasized here that a similar stabilizing effect is found also in the case of non-uniform gravity in which the gravitational acceleration, g, decreases with height, such as in a point mass potential adopted by Matsumoto et al. (1988). This is because small g is equivalent to high temperature, T, since the instability wavelength is in proportion to the pressure scale height, $H \propto T/g$. In the simulation model of Matsumoto et al. (1988), the parameter $\epsilon = (GM/R)/[(1+1/\beta){C_s}^2]$ is assumed to be 6. This value is much smaller than that expected for thin accretion disks and actual galactic disks, $\epsilon \sim 1000$. For this reason, this model was claimed to

be irrelevant to real phenomena (e.g., Mouschovias 1996 private communication). However, considering the equivalence of small g and high T, the Matsumoto et al. model is effectively the same as that of a disk with a hot corona. This has been confirmed later by more realistic simulations (e.g., Shibata et al. 1990b). Hence the reader can safely apply the Matsumoto et al. (1988, 1990) results to real phenomena if he/she normalizes the length scale by the local pressure scale height in the disk (not by the radius of the disk).

Finally, it should be emphasized that the stabilizing effect of the corona works not only in the linear regime but also in the nonlinear regime. In fact, the ratio of the coronal pressure to the disk (or photospheric) pressure, p_{cor}/p_{ph} (or equivalely p_∞/p_{disk}), is very important for the nonlinear evolution of the Parker instability. If p_{cor}/p_{ph} (or p_∞/p_{disk}) is much smaller than unity, the upper part of the expanding magnetic loop cannot stop as long as p_{cor} is smaller than the magnetic pressure of the expanding loop. In this case, the expanding loop shows a self-similar evolution (Shibata et al. 1989a,b, 1990, and also section 4.2.1).

4.1.4. *Effect of Rotation and Shearing Motion*

Chou et al. (1995) performed 3D MHD simulations to study the effect of the Coriolis force on the nonlinear evolution of the Parker instability of an isolated magnetic flux tube in the isothermal gas layer which is rotating rigidly at angular speed Ω. They found that the rising magnetic flux tube is twisted by the Coriolis force to form a globally twisted flux tube (Fig. 11). This mechanism explains the observed tilt of bipolar sunspot groups.

Shibata and Matsumoto (1991), on the other hand, noted that the local twist may be generated in the downflow along the rising magnetic loop in addition to the global twist, since the downflowing blob or cloud contracts during the course of the downflow and suffer from the Coriolis force, similar to the usual contracting clouds in our Galaxy (Fig. 12). The sense of the rotation of the contracting cloud is the same as that of the rotation of the Galaxy. The twist accumulates in the valley of the undulating magnetic field lines, where the giant molecular cloud is formed. They applied this mechanism to explain the helical magnetic twist observed in a giant molecular cloud in the Galaxy (Uchida et al. 1990). Turbulent magnetic fields often observed in the valley of undulating magnetic fields (e.g., M31, see Beck et al. 1989) may also be explained by this mechanism. The twisted magentic field thus created is, in turn, favorable for the formation of the large scale cloud complex since the twist (magnetic shear) stabilizes the small scale interchange mode (Hanawa et al. 1992). It should be noted here that *the direction of this local twist in the rising magnetic loop is opposite to that of the global twist.* Hence, this mechanism may explain the origin

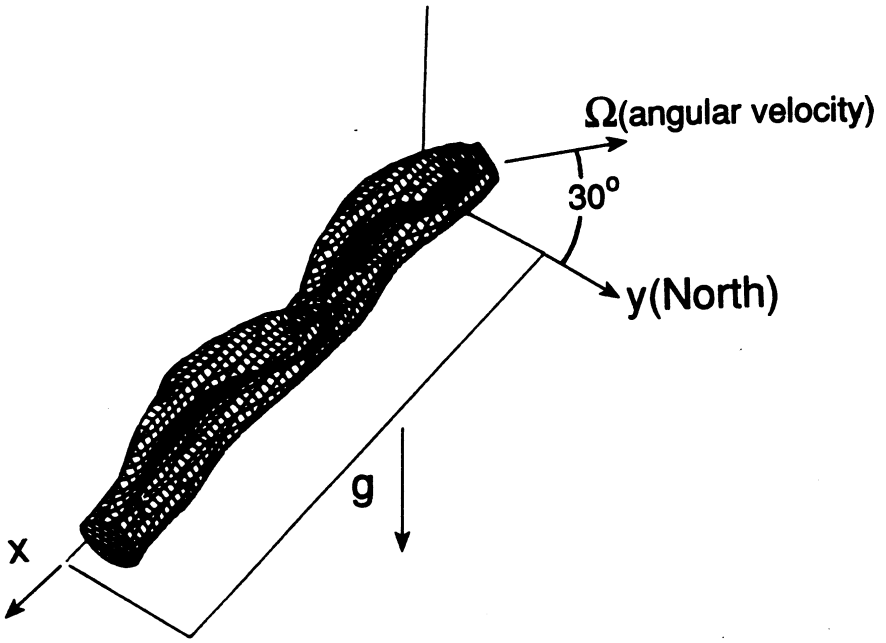

Figure 11. Twisted flux tube formed by the nonlinear evolution of the Parker instability in the presence of the Coriolis force (Chou et al. 1995).

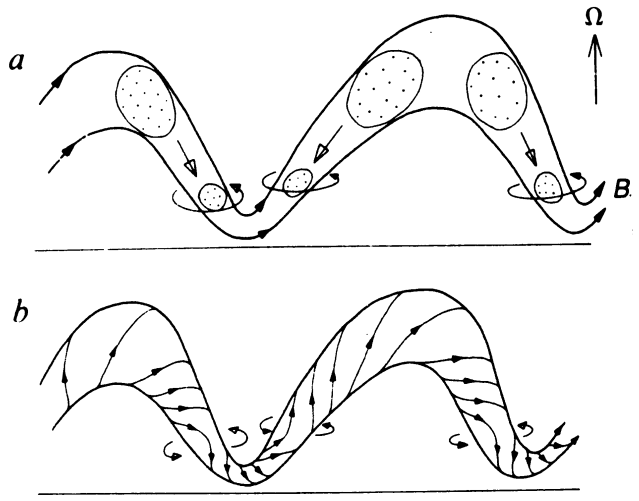

Figure 12. The formation of local twist by the effect of the Coriolis force on a contracting downflowing blob (or cloud) (Shibata and Matsumoto 1991).

of the magnetic twist observed in solar active regions (Pevtsov et al. 1994) and filaments (Rust 1994).

In actual rotating systems, there is a shear flow, i.e., differential rotation. What is the effect of a shearing flow on the Parker instability ? Shibata, Tajima, and Matsumoto (1990) studied this effect in a situation such that the horizontal magnetic flux (which is unstable to the Parker instability if there is no shear flow) is suffering from an amplification by the shear flow in an accretion disk. Usually the field amplification by the shear flow leads to instability or loss of equilibrium (as is well known in theoretical

research of solar flares). However, against expectations, this case leads to an effective *stabilization* of the Parker instability, since the shearing time scale is shorter than the Parker time scale. As a result of this dynamic stabilization, the magnetic field cannot escape from the disk, and hence the disk evolves into the *low* β disk in which various violent phenomena (such as flares) can oocur *inside* the disk. On the other hand, if the shearing effect is weak, the magnetic flux can rapidly escape from the disk to form a high β disk, similarly to the conventional picture of an accretion disk. In this case, the disk-corona structure may be similar to the solar interior-corona structure. Shibata et al. (1990b) discussed the possibility of these two types of accretion disks, *low* β disk and *high* β disk. Recently, Mineshige et al. (1995) applied this idea to the observed two states of accretion disks, a low state and a high state (e.g., Miyamoto et al. 1995), and proposed that low states correspond to the *low* β disk. (As for a linear stability analysis of the Parker instability in a shearing flow parallel to the magnetic field, see Fogglizo and Tagger (1994).)

The shearing motion, on the other hand, can have a destabilizing effect [5] on a magnetized gas layer, i.e. a magneto-rotational instability (or Velikhov-Chandrasekhar instability or Balbus-Hawley instability). This instability gives one answer on the origin of viscosity in the accretion disk (e.g., Hawley, Gammie, and Balbus 1995, Matsumoto and Tajima 1995, Brandenberg et al. 1995). Since this instability occurs in wavelengths shorter than the Parker unstable wavelength, many interesting questions arise. Once this instability develops, does the disk magnetic field become turbulent and have only short scales ? In that case, is the Parker instability completely suppressed ? If the initial magnetic field is not so weak as in the case of star forming regions, what will happen ? The nonlinear coupling between the magneto-rotational instability and the Parker instability in realistic 3D situations will be an interesting and important subject for the future.

4.2. EMERGING SOLAR MAGNETIC LOOPS

4.2.1. *Self-similar Expansion of Magnetic Loops*

In the last subsection, we have considered the evolution of the periodic perturbation in the Parker instability. What is the result of non-periodic perturbations ? In other words, what is the effect of side boundaries ? Shibata et al. (1989a) studied this effect for the Parker instability occurring in the isolated magnetic flux sheet embedded in the solar photosphere in order to make a model of emerging magnetic loop. (Note that emerging

[5] Even the Parker instability can be nonlinearly excited by the shearing motion when the gas layer is linearly stable (Kaisig et al. 1990).

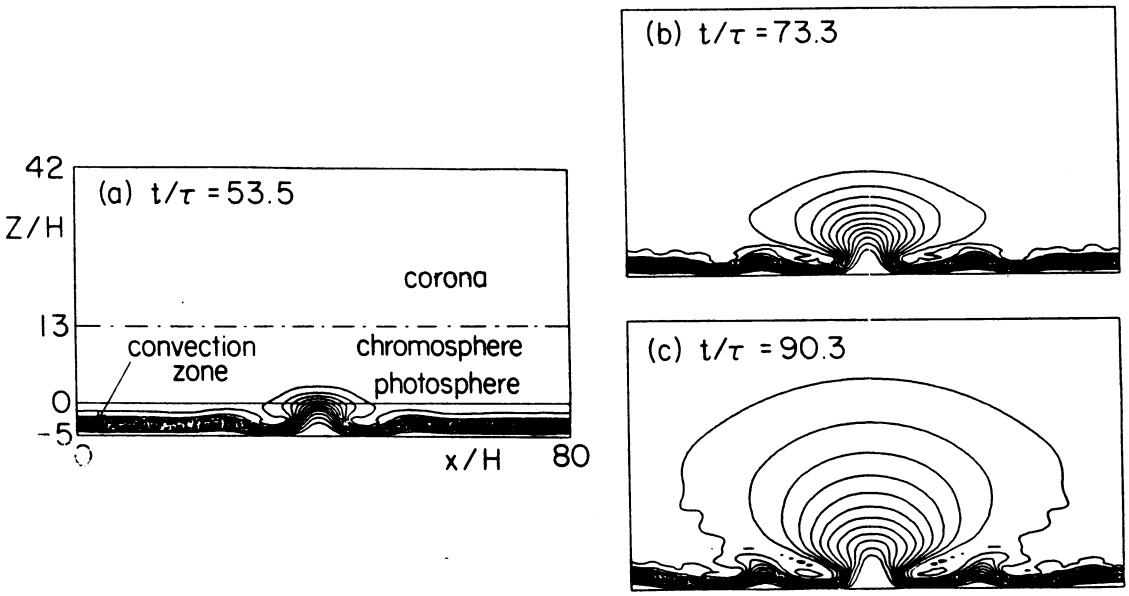

Figure 13. The self-similar evolution of the expanding magnetic loop as a result of the nonlinear evolution of the Parker instability (Shibata et al. 1990).

loops in the Sun are not periodic, at least, in the scale of active regions.) One important difference from the previous Matsumoto et al. model (1988, 1990) is that in the solar case the coronal pressure is much smaller than the photospheric pressure, $p_{cor}/p_{ph} \sim 10^{-7}$, so that the coronal pressure cannot work as a nonlinear stabilizing agent. Assuming a localized perturbation with the most unstable wavelength λ_{max}, Shibata et al. (1989a) compared the nonlinear evolution of the following three different cases; (1) $X_{max} = \lambda_{max}$, (2) $X_{max} = 2\lambda_{max}$, and (3) $X_{max} = 4\lambda_{max}$, where X_{max} is the horizontal box size.

They found that as X_{max} increases, the magnetic loop expands more horizontally. As a result, the magnetic tension force becomes smaller, so that the loop can continue to expand to upward direction and finally the expansion becomes approximately self-similar in the case of $X_{max} \geq 4\lambda_{max}$ (Fig. 13). Such self-similar behaviors are more clearly seen in a one dimensional distribution of the physical quantities along the height at the midpoint of the magnetic loop (Fig. 14). From this plot, we find

$$V_z \simeq \omega_n z,$$

$$\rho \propto z^{-4}, \qquad B_x \propto z^{-1}.$$

Here ω_n is the *nonlinear growth rate* in the Lagrangian frame in which the velocity increases with time as $V_z \propto \exp(\omega_n t)$. Interestingly, this *nonlinear growth rate* is found to be related to the linear growth rate ω of the Parker instability;

$$\omega_n \simeq \omega/2.$$

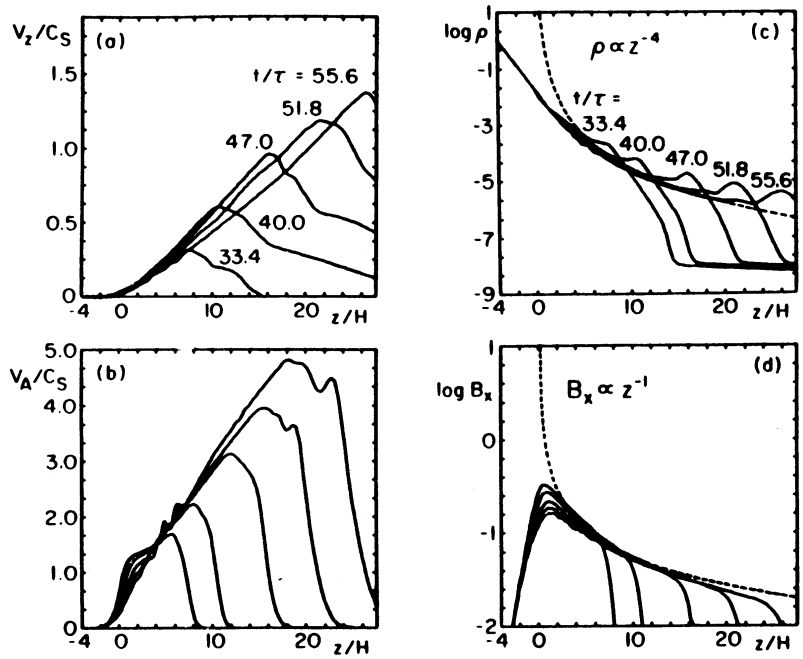

Figure 14. 1D distribution (in z) of physical quantities at the midpoint of the magnetic loop which is expanding self-similary as a result of the nonlinear evolution of the Parker instability (Shibata et al. 1989a). The times are in unit of $\tau = C_s/H$.

This relation holds in various situations, such as in the cases of the Parker-convective instability (Nozawa et al. 1992) and the Parker instability coupled with interchange modes (Matsumoto et al. 1993). We also find that the Alfven speed in the rising loop increases with height. This means that the plasma β decreases with height and explains why we have a low β corona in magnetic loops. As a magnetic loop expands, it tends to be current free since both thermal and gravitational forces become smaller than the magnetic force as the loop rises. Although Shibata et al. (1989a) found these results assuming an isolated magnetic flux initially, almost the same results are found by assuming continuous magnetic field distribution as an intitial condition (Kamaya et al. 1996a).

Shibata et al. (1989a) found an approximate self-similar solution for this problem, which explains these nonlinear simulation results very well (see also Shibata, Tajima, Matsumoto (1990a) for a detailed self-similar analysis and physical interpretation).

These results explain many observational characteristics of the emerging magnetic flux in the solar atmosphre (Shibata et al. 1989b). For example, the observations show that the rise velocity of the magetic loop in the photosphre ($z < 400$ km) is of order of 1 – 2 km/s, while the loop expands at 10 – 20 km/s in the upper chromosphere ($z \sim 4000 - 6000$ km). This is nicely explained by the equation found from the simulations and theory,

$$V_z \simeq \omega_n z \sim 0.06\, C_s(z/H) \sim 12\ (z/4000\ \mathrm{km})\ \mathrm{km/s}.$$

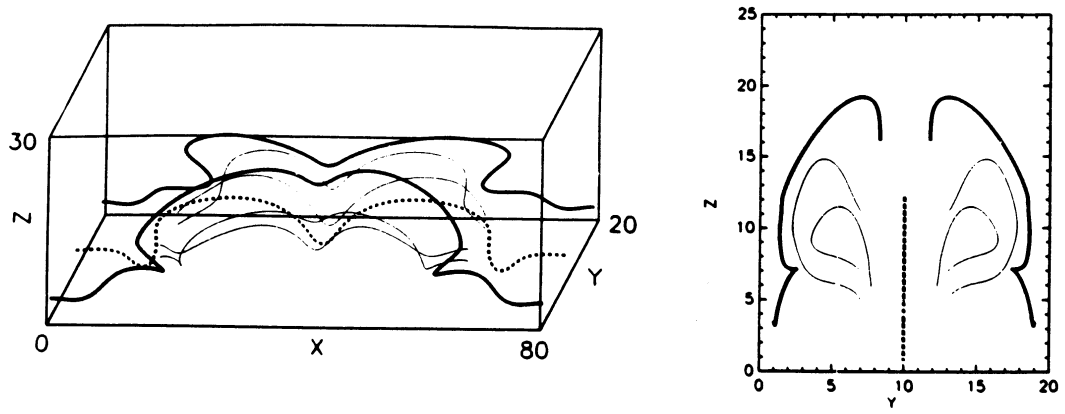

Figure 15. The 3D Parker instability coupled with interchnge mode (Matsumoto et al. 1993). Left: Magnetic field lines in 3D space. Right: Field lines in $y - z$ plane.

Observations also show that the downflow occurs at 30 – 50 km/s along the rising loops in the upper chromosphere, which is again explained by these simulation results.

4.2.2. *Three Dimensional Effect: Coupling with the Interchange Modes*

What will happen to the nonlinear evolution of the Parker instability in real 3D space ? In 3D space, the interchange mode can couple with the undular (Parker) mode. Matsumoto and Shibata (1992) and Matsumoto et al. (1993) studied this effect with full 3D simulations, and found that the resulting magnetic structure is a *interleaved structure* for both the galactic and the solar cases. It is also found that the *vortex motion* occurs around the rising magnetic loops, which produce *magnetic twist* or *torsional Alfven waves* (Fig. 15). Interestingly, even with such interleaved structure, the overall dynamics such as the self-similar expansion, is similar to that found from 2D simulations.

Matsumoto et al. (1993) also studied a 3D evolution of the emergence of the isolated magnetic flux tube, and found that the tube expands not only to the upward direction but also to the horizontal direction perpendicular to the tube. Such horizontal expansion decreases internal magnetic pressure significantly, and so the rise motion of the tube tends to be suppressed when the tube size (or the total magnetic flux of the tube) is smaller. It is found that there is a threshold magnetic flux for the tube to rise into the corona, which is about 0.3×10^{20}Mx. Interestingly, this agrees with observationally known threshold flux for the formation of arch filament system (e.g., Zwaan 1987).

4.2.3. *Emergence of Twisted Flux Tube*

Observations (Kurokawa 1989, Leka 1994) show that in some active regions the emerging flux is already twisted before emergenece. Matsumoto et al. (1996b) studied the nonlinear evolution of the coupling of the Parker instability with the kink instability as a model of emergence of a twisted flux tube. They found that the resulting magnetic flux tube show the double helix pattern and that their results eplain various observations such as the peculiar proper motion of sunspots and the apparent sheared S structure of coronal loops found by *Yohkoh*.

5. Flares – Magnetic Reconnection

5.1. SOLAR COMPACT FLARES AND X-RAY JETS

As we have seen above, a magnetic loop rapidly emerges from below the photosphere to the corona due to the Parker instability. Since the corona is filled with strong magnetic fields (i.e., low β plasma), such emerging magnetic loop would interact with pre-existing magnetic fields. What is the consequence of such interaction ? As an extention of previous emerging flux models (Shibata et al. 1989a,b, 1990c), Shibata, Nozawa, and Matsumoto (1992) first studied this process, i.e., the interaction between emerging flux and overlying anti-parallel horizontal coronal field, by performing high resolution 2D MHD simulations. They assumed a simplified anomalous resistivity model such that $\eta \propto (v_d - v_c)^2$ where $v_d = j/\rho$ is the drift velocity of the current j, and v_c is the critical velocity above which the anomalous resistivity sets in (Sato and Hayashi 1979, Ugai 1986). Their findings are as follows. Multiple magnetic islands are first created by the tearing instability in the current sheet between the emerging flux and the coronal field. These islands coalesce with each other by the coalescence instability, and are ejected out of the current sheet at high speed (of order of Alfven speed). The total energy released in this process is $\sim 10^{28} - 10^{29}$ ergs, comparable to that of compact solar flares. (This is an extension of the Heyvaerts et al. (1977)'s emerging flux flare model, and also of numerical simulations by Forbes and Priest (1984).) [6]

Yokoyama and Shibata (1994, 1995, 1996a,b; Yokoyama 1995) further developed this model, by performing comprehensive parameter survey, and extended the model to various situations.

(1) They succesfully modeled the X-ray jets which are recently found by *Yohkoh* (Shibata et al. 1992b, 1994, Strong et al. 1992, Shimojo et al.

[6] As for a model of larger flares (e.g., Tsuneta et al. 1992, Shibata 1995), different approaches may be necessary; one such kind of modeling has been done by Magara et al. (1995).

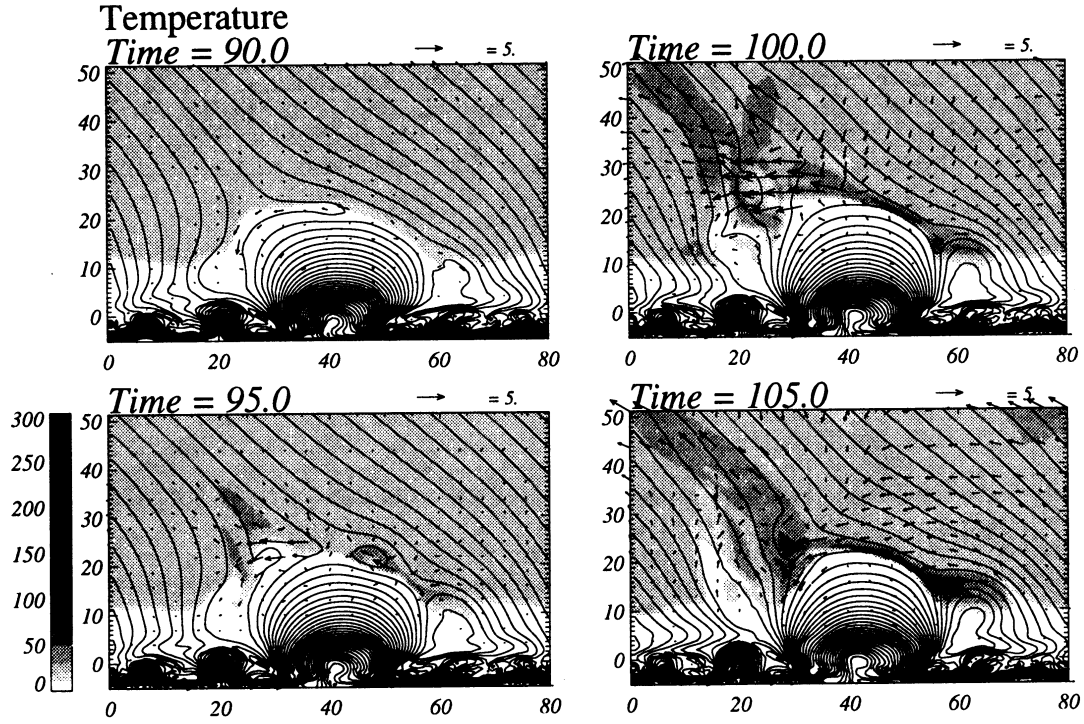

Figure 16. Magnetic reconnection driven by the emerging flux as a result of the Parker instability in the case of an oblique coronal field (Yokoyama and Shibata 1995a,b).

1995) by the emerging flux reconnection model (Yokoyama and Shibata 1995, 1996a,b). Figure 16 illustrates one typical example in which the initial coronal field is assumed to be oblique. Although the physical processes around the current sheet are similar to those found by Shibata et al. (1992a), it is found in this case that the magnetic islands (plasmoids) containing cool dense plasma are ejected sideway by the magnetic tension force, showing a whip-like motion. This is similar to the observed motion of Hα surges (e.g., Kurokawa and Kawai 1993, Canfield et al. 1995). Both plasmoids and the reconnection jets collide with the ambient oblique field (in the left side) to excite the fast mode MHD shock at the colliding point. The plasmoids disappear due to secondary reconnection with the oblique field, and the reconnection jets are decelerated significantly. However, plasmas behind the shock are accelerated again along the oblique field lines by the enhanced gas pressure behind the shock, and form a large scale hot jet which may correspond to observed X-ray jets. This model predicts coexistence of the hot and cool jets, and thus could explain observed coexistence of X-ray jets and Hα surges in some cases (Shibata et al. 1992b, Canfield et al. 1995, Okubo et al. 1995).

(2) Yokoyama and Shibata (1994), on the other hand, studied the basic physics of reconnection. They compared a *uniform resistivity* model with an *anomalous resistivity* model (similar to above Shibata et al. (1992a)'s

model) in reconnection driven by the Parker instability, and found that in the *uniform resistivity* model, the reconnection is slow and tends to be steady Sweet-Parker type, while in the *anomalous resistivity* model, it is fast and becomes nonsteady Petschek type, in agreement with Ugai (1995). In the *anomalous resistivity* case, it is also found that the formation and ejection of plasmoids are key processes, and that if the threshold of anomalous resistivity becomes higher, the reconnection becomes faster and more vilolent once reconnection occurs.

5.2. PROTOSTELLAR MAGNETOSPHERE

Hirose et al. (1995, Hirose 1994) studied the reconnection between a (non-rotating) protostellar bipolar magnetic field and poloidal magnetic fields carried by an accretion disk, as an extension of the previous Uchida-Shibata (1984, 1985) model for protostellar jets. They found that the reconnection itself accelerates plasmas directly from the disk, in addition to the general acceleration of disk plasmas via the $\mathbf{J} \times \mathbf{B}$ force (centrifugal force and magnetic pressure gradient force of toroidal fields). They suggested that optical jets may be generated by this reconnection acceleration. This reconneciton process is important to understand the evolution of protostellar rotation, and hence in the future the interaction between a *rotating* protostellar magnetosphere and a magnetized accretion disk should be studied in more detail.

6. Future Directions

In the following, I will summarize some future important subjects of *numerical solar and astrophysical MHD* in relation to jets, loops, and flares.

(1) Three dimensional MHD numerical simulations of magnetically driven jets from accretion disks should be studied from various points of view. If the initial poloidal field is weak, the Balbus-Hawley instability will modify the initial field significantly in the disk. Near the surface of the disk, the magnetic field lines are highly wound up, producing strong toroidal fields, which would be unstable to a non-axisymmetric instability such as the Parker instability. The magnetic reconnection in association with these instabilities will be very important. The 3D stability as well as long term behavior of the magnetically driven jet should also be studied in detail.

(2) In the case of the Parker instability in galactic disks, the effect of cosmic rays should be incorporated as emphasized by Parker (1966, 1979). Cosmic rays enable the nonlinear evolution of the Parker instability to proceed more vigorously. The effect of the Coriolis force and shearing motion on the nonlinear Parker instability should also be studied in detail with

high resolution 3D simulations, in relation to the formation of magnetic twist in various scales. The magnetic reconnection and resulting plasma heating will also be important in galactic disks and halos.

(3) In the case of the Sun, the generation and emergence of twisted flux tubes and resulting 3D reconnection would be one of the central problems in relation to the origin of flares. Since there are a lot of observational data for the solar case (such as *Yohkoh* data), it would be important to develop more realistic models incorporating various physical processes, such as heat conduction, evaporation, and radiative cooling (Hori et al. 1995), into the reconection problem (Yokoyama 1995).

References

Basu, S., Mouschovias, T. Ch., and Paleologou, E, V., 1996, *Astrophys. Lett. and Comm.*, in press.

Beck, R., et al., 1989, *A. Ap.*, **222**, 58.

Balbus, S. A., and Hawley, J. F., 1991, *Ap. J.*, **376**, 214.

Burgarella, D., Livio, M., and O'Dea, C. P. (eds), 1993, *Astrophysical Jets*, Cambridge Univ. Press.

Blandford, R. D., and Payne, D. G., 1982, *MNRAS*, **199**, 883.

Blandford, R. D., 1993, in *Astrophysical Jets*, eds. Burlarella, D. et al., Cambridge Univ. Press, p. 15.

Brandenburg, A., Nordlund, A., Stein, R. F., and Torkelsson, U., 1995, *Ap. J.*, **446**, 741.

Canfield, R. C., Reardon, K. P., Leka, K. D., Shibata, K., Yokoyama, T., and Shimojo, M., 1995, *Ap. J.*, submitted.

Cao, X., and Spruit, H. C., 1994, *A. Ap.*, **287**, 80.

Chou, W., Tajima, T., Matsumoto, R., and Shibata, K., 1996, *Proc. IAU Colloq. No. 153*, in press.

Colgate, S. A., and White, R. H. 1967, *Ap. J.*, **143**, 626.

Fogglizo, T., and Tagger, M., 1994, *A. Ap.*, **287**, 297.

Forbes, T. G., and Priest, E. R., 1984, *Solar Phys.*, **94**, 315.

Giz, A. T., and Shu, F. H. 1993, *Ap. J.*, **404**, 185.

Haisch, B., Strong, K. T., and Rodono, M., 1991, Ann. Rev. A. Ap., **29**, 275.

Hanawa, T., Matsumoto, R., and Shibata, K., 1992, *Ap. J. Lett.*, **393**, L71.

Hawley, J. F., Gammie, C. F., and Balbus, S. A., 1995, *Ap. J.*, **440**, 742.

Heyvaerts, J., Priest, E. R., and Rust, D. M.: 1977, *Ap. J.*, **216**, 123.

Heyvaerts, J., and Norman, C., 1989, *Ap. J.*, **347**, 1055.

Hirose, S., 1994, Ph. D. Thesis, University of Tokyo.

Hirose, S., et al., 1995, to be submitted.

Hollweg, J., 1982, *Ap. J.*, **257**, 345.

Hollweg, J., 1992, *Ap. J.*, **389**, 731.

Hollweg, J., Jackson, S., and Galloway, D., 1982, *Solar Phys.*, **75**, 35.

Hori, K., Yokoyama, T., Kosugi, T., and Shibata, K., 1996, *Proc. IAU Colloq. 153*, in press.

Horiuchi, T., Matsumoto, R., Hanawa, T. and Shibata, K., 1988, *Publ. Astron. Soc. Japan*, **40**, 147.

Hughes, D. W., and Procter, M. R. E. 1988, *Ann. Rev. Fluid Mech.*, **20**, 187.

Kaisig, M., Tajima, T., Shibata, K., Nozawa, S., and Matsumoto, R., 1990, *Ap. J.*, **358**, 698.

Kamaya, T., Mineshige, S., Matsumoto, R., Shibata, K., 1996a, *Ap. J. Lett.*, in press.

Kamaya, T., Mineshige, S., Matsumoto, R., Hanawa, T., Shibata, K., 1996b, (in prepa-

ration).
Kudoh, T., and Shibata, K., 1995, *Ap. J. Lett.*, **452**, L41.
Kudoh, T., and Shibata, K., 1996a, *Astrophys. Lett. and Comm.*, in press.
Kudoh, T., and Shibata, K., 1996b, *Ap. J.*, (to be submitted).
Kurokawa, H., 1989, *Space Sci Rev.*, **51**, 49.
Kurokawa, H., and Kawai, G. 1993, *Proc. IAU Colloq. No. 141, ASP Conference Series 46*, ed. H. Zirin, G. Ai, and H. Wang, pp. 507-510.
Leka, K. D., 1994, Ph. D. Thesis, Hawaii Univ.
Lovelace, R. V. E., Berk, H. L., and Contopoulos, J., 1991, *Ap. J.*, **379**, 696.
Magara, T., Mineshige, S., Yokoyama, T., and Shibata, K., 1995, *Ap. J.*, submitted.
Matsumoto, R., Horiuchi, T., Shibata, K., and Hanawa, T., 1988, *Publ. Astron. Soc. Japan*, **40**, 171.
Matsumoto, R., Horiuchi, T., Hanawa, T., and Shibata, K., 1990, *Ap. J.*, **356**, 259.
Matsumoto, R., and Shibata, K., 1992, *Publ. Astr. Soc. Japan*, **44**, 167.
Matsumoto, R., Tajima, T., Shibata, K., and Kaisig, M., 1993, *Ap. J.*, **414**, 357.
Matsumoto, R., and Tajima, T., 1995, *Ap. J.*, **445**, 767.
Matsumoto, R., Uchida, Y., Hirose, S., Shibata, K., Hayashi, M. R., Ferrari, A, Bodo, G., and Norman, C., 1996a, *Ap. J.*, in press.
Matsumoto, R., Tajima, T., Chou, W., and Shibata, K., 1996b, *Proc. IAU Colloq. No. 153*, in press.
Michel, F. C., 1969, *Ap. J.*, **158**, 727.
Mineshige, S., Kusunose, M., Matsumoto, R., 1995, *Ap. J. Lett.*, **445**, L43.
Miyamoto, M., Kitamoto, S., Hayashida, K., and Egoshi, W., 1995, *Ap. J. Lett.*, **442**, L13.
Moreno-Insertis, F., 1986, *A. Ap.*, **166**, 291.
Moriarty-Schieven, G. H., and Wannier, P. G., 1991. *Ap. J.*, **373**, L23.
Mouschovias, T. Ch., 1974, *Ap. J.*, **192**, 37.
Mouschovias, T. Ch., 1996, in *Solar and Astrophysical MHD Flows*, K. Tsinganos (ed.), Kluwer, in press.
Nozawa, S., Shibata, K., Matsumoto, R., Tajima, T., Sterling, A. C., Uchida, Y., Ferrari, A., and Rosner, R., 1992, *Ap. J. Suppl.*, **78**, 267.
Ohno, Y., Sakashita, S., and Ohyama, N., 1961, *Prog. Theor. Phys. Suppl.*, **20**, 85.
Okubo, A., et al., 1996, *Proc. IAU Colloq. 153*, in press.
Osterblock, D. E., 1961, *Ap. J.*, **134**, 347.
Parker, E. N., 1966, *Ap. J.*, **145**, 811.
Parker, E. N., 1979, *Cosmical Magnetic Field* (Clarendon Press, Oxford), p. 314.
Pevtsov, A. A., Canfield, R. C., and Metclaf, T. R., 1994, *Ap. J. Lett.*, **425**, L117.
Pudritz, R. E. and Norman, C., 1986, *Ap. J.*, **301**, 571.
Priest, E. R.: 1982, *Solar Magnetohydrodynamics*, Reidel Pub., Dordrecht.
Rust, D. M., 1994, *Geophys. Res. Lett.*, **21**, 241.
Sakurai, T., 1987, *Publ. Astron. Soc. Japan*, **39**, 821.
Sato, T., and Hayashi, T., 1979, *Phys. Fluids*, **22**, 1189.
Sauty, C., and Tsinganos, K., 1994, *Astron. Ap.*, **287**, 893.
Schüssler, M., 1996, in *Solar and Astrophysical MHD Flows*, K. Tsinganos (ed.), Kluwer, in press.
Shibata, K., 1983, *Publ. Astron. Soc. Japan*, **35**, 263
Shibata, K., 1996, *Adv. Space Res.*, **17**, (4/5)9.
Shibata, K., Nishikawa, T., Kitai, R. and Suematsu, Y., 1982, *Solar Phys.*, **77**, 121.
Shibata, K., and Suematsu, Y., 1982, *Solar Phys.*, **78**, 333.
Shibata, K., and Uchida, Y., 1985, *Publ. Astron. Soc. Japan*, **37**, 31.
Shibata, K., and Uchida, Y., 1986a, *Publ. Astron. Soc. Japan*, **38**, 631.
Shibata, K., and Uchida, Y., 1986b, *Solar Phys.*, **103**, 299.
Shibata, K., and Uchida, Y., 1987, *Publ. Astron. Soc. Japan*, **39**, 559.
Shibata, K., et al., 1989a, *Ap. J.*, **338**, 471.
Shibata, K., Tajima, T., Steinolfson, R. and Matsumoto, R., 1989b, *Ap. J.*, **345**, 584.

Shibata, K., and Uchida, Y., 1990, *Publ. Astron. Soc. Japan*, **42**, 39.
Shibata, K., Tajima, T., and Matsumoto, R., 1990a, *Phys. Fluids*, **B2**, 1989.
Shibata, K., Tajima, T., and Matsumoto, R., 1990b, *Ap. J.*, **350**, 295.
Shibata, K., Nozawa, S., Matsumoto, R., Sterling, A. C., and Tajima, T., 1990c, *Ap. J. Lett.*, **351**, L25.
Shibata, K., and Matsumoto, R. 1991, *Nature*, **353**, 633.
Shibata, K., Nozawa, S., and Matsumoto, R., 1992a, *Publ. Astr. Soc. Japan*, **44**, 265.
Shibata, K., et al., 1992b, *Publ. Astr. Soc. Japan Letters*, **44**, L173.
Shibata, K., et al., 1994, *Ap. J. Lett.*, **431**, L51.
Shimojo, M., Hashimoto, S., Shibata, K., Hirayama, T., Hudson, H., and Acton, L., 1995, *Publ. Astr. Soc. Japan*, in press.
Shu, F. H., Adams, F. C., and Lizano, S., 1987, *Ann. Rev. A. Ap.*, **25**, 23.
Sofue, Y., and Handa, T., 1984, *Nature*, **310**, 568.
Sterling, A. C., and Hollweg, J. V., 1988, *Ap. J.*, **327**, 950.
Sterling, A. C., Shibata, K., Mariska, J. T., 1993, *Ap. J.*, **407**, 778.
Stone, J. M., and Norman, M., 1994, *Ap. J.*, **433**, 746.
Strong, K. T. et al., 1992, *Publ. Astr. Soc. Japan*, **44**, L161.
Suematsu, Y., Shibata, K., Nishikawa, T. and Kitai, R., 1982, *Solar Phys.*, **75**, 99.
Tajima, T., 1989, *Computational Plasma Physics*, Addison Wesley.
Todo, Y., Uchida, Y., Sato, T., and Rosner, R., 1992, *Publ. Astron. Soc. Japan*, 44, 245.
Todo, Y., Uchida, Y., Sato, T., and Rosner, R., 1993, *Ap. J.*, 403, 164.
Tsinganos, K., and Trussoni, A. A., 1991, *Astron. Ap.*, **249**, 156.
Tsinganos, K., Surlantzis, G., and Priest, E. R., 1993, *Astron. Ap.*, **275**, 613.
Tsinganos, K. et al., 1996, in *Solar and Astrophysical MHD Flows*, K. Tsinganos (ed.), Kluwer, in press.
Tsuneta, S., et al., 1992, *Publ. Astr. Soc. Japan*, **44**, L63.
Uchida, Y., and Shibata, K., 1984, *Publ. Astron. Soc. Japan*, **36**, 105.
Uchida, Y., and Shibata, K., 1985, *Publ. Astron. Soc. Japan*, **37**, 515.
Uchida, Y., Shibata, K. and Sofue, Y., 1985, *Nature*, **317**, 699.
Uchida, Y., et al., 1987, *Publ. Astron. Soc. Japan*, **39**, 907.
Uchida, Y., Mizuno, A., Nozawa, S., and Fukui, Y., 1990, *Nature*, **42**, 69.
Uchida, Y., Todo, Y., Rosner, R. and Shibata, K., 1992, *Publ. Astr. Soc. Japan*, **44**, 227.
Ugai, M., 1986, *Phys. Fluids*, **29**, 3659.
Ugai, M., 1995, *Phys. Plasmas*, **2**, 388.
Ulmschneider, P., Priest, E. R., and Rosner, R. (eds.), 1991, *Mechanisms of Chromospheric and Coronal Heating*, Springer Verlag.
Ustyugova, G. V., et al., 1995, *Ap. J. Lett.*, **439**, L39.
Yokoyama, T., 1995, Ph. D. Thesis, National Astronomical Observatory.
Yokoyama, T., and Shibata, K., 1994, *Ap. J. Lett.*, **436**, L197.
Yokoyama, T., and Shibata, K., 1995, *Nature*, **375**, 42.
Yokoyama, T., and Shibata, K., 1996a, *Astrophys. Lett. and Comm.*, in press.
Yokoyama, T., and Shibata, K., 1996b, *Publ. Astron. Soc. Japan*, in press.